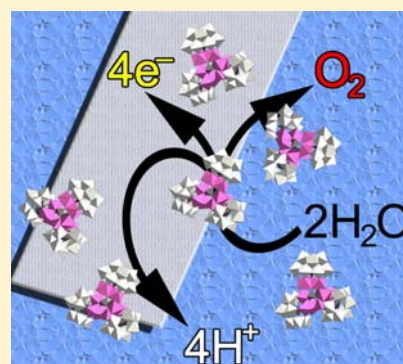


Identification of a Nonanuclear $\{\text{Co}^{\text{II}}_9\}$ Polyoxometalate Cluster as a Homogeneous Catalyst for Water OxidationSara Goberna-Ferrón,[†] Laura Vígara,[†] Joaquín Soriano-López,[†] and José Ramón Galán-Mascarós^{*,†,‡}[†]Institute of Chemical Research of Catalonia (ICIQ), Avenida Països Catalans 16, E-43007 Tarragona, Spain[‡]Catalan Institution for Research and Advanced Studies, Passeig Lluís Companys 23, E-08010 Barcelona, Spain

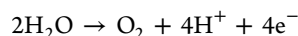
Supporting Information

ABSTRACT: The polyanion of formula $\{\text{Co}_9(\text{H}_2\text{O})_6(\text{OH})_3(\text{HPO}_4)_2(\text{PW}_9\text{O}_{34})_3\}^{16-}$ (Co_9) contains a central nonacobalt core held together by hydroxo and hydrogen phosphate bridges and supported by three lacunary Keggin-type polyphosphotungstate ligands. Our data demonstrate that Co_9 is a homogeneous catalyst for water oxidation. Catalytic water electrolysis on fluorine-doped tin oxide coated glass electrodes occurs at reasonable low overpotentials and rates when Co_9 is present in a sodium phosphate buffer solution at neutral pH. We carried out our experiments with an excess of 2,2'-bipyridyl as the chelating agent for free aqueous Co^{II} ions, in order to avoid the formation of a cobalt oxide film on the electrode, as observed for other polyoxometalate catalysts. In these conditions, no heterogeneous catalyst forms on the anode, and it does not show any deposited material or significant catalytic activity after a catalytic cycle. Co_9 is also an extremely robust catalyst for chemical water oxidation. It is able to continuously catalyze oxygen evolution during days from a buffered sodium hypochlorite solution, maintaining constant rates and efficiencies without any significant apparition of fatigue.



INTRODUCTION

Water oxidation catalysis is one of the biggest challenges that inorganic chemistry is facing today. The discovery of a fast, robust, and readily available catalyst would be key for the realization of artificial photosynthesis, an achievement that could probably solve the energy problem worldwide.¹ Oxygen evolution from water is a complex redox process. It occurs at high oxidation potentials, and it involves four electrons. An active catalyst for such a high-energy multielectron process will probably² need the participation of metal ions, as occurs in natural photosynthesis.³



$$E = +1.229 - 0.059(\text{pH}) \text{ V vs NHE at } 25^\circ\text{C} \quad (1)$$

Several heterogeneous water oxidation catalysts (WOCs) have been known for many years.⁴ Oxides and hydroxides of transition metals show catalytic activity and, in some cases, long-term stability.⁵ The straightforward preparation of these WOCs has allowed for their easy incorporation into devices.⁶ On the latter, the most remarkable result has been the incorporation of an electrodeposited phosphate oxide cobalt layer (Pi-Co) onto the anode of a silicon-based solar cell.⁷ This "artificial leaf" is able to split water by direct irradiation with sunlight working at neutral pH.⁸ Regarding industrial applications, this Pi-Co WOC shows a pH-dependent degradation with time,⁹ making the artificial leaf, at the moment, too costly to compete with other hydrogen production procedures.

Homogeneous WOCs are less stable than their solid-state counterparts, but, on the other hand, they allow for a better understanding of the reaction mechanisms and easier optimization.¹⁰ The most studied molecular WOCs have been ruthenium complexes,¹¹ since the discovery of Meyer's original "blue dimer",¹² where two Ru ions are bound through oxo bridges and coordinated by polypyridyl ligands. Many other ruthenium complexes with different nuclearity have shown high catalytic activity.¹³ Iridium organometallic complexes are also efficient WOCs.¹⁴ Because ruthenium and iridium are precious metals, these catalysts do not meet one of the crucial requirements for a technologically relevant WOC: inexpensive starting materials. First-row transition-metal complexes with coordination geometries analogous to those of ruthenium-based WOCs have also shown significant catalytic activity, with examples found in cobalt,¹⁵ iron,¹⁶ manganese,^{17,18} and copper¹⁹ chemistry. Still, these candidates lack long-term stability, usually related to the presence of organic ligands. Organic ligands are needed for the formation of the complexes, but they are unstable toward oxidative deactivation in water oxidation conditions.

There is an important problem in the characterization of true homogeneous catalysts. Many of them are precursors for metal oxides, which can also act as WOCs. If the corresponding oxides form in water oxidation conditions, the activity of the molecular precursors can be questioned.²⁰ This is even more important in the case of electrocatalysis. The anode surface can

Received: July 24, 2012

Published: October 18, 2012

promote decomposition of the homogeneous species into an active electrodeposited material.²¹ It is crucial to discard the participation of any decomposition product in the characterization of new, or old, WOCs. The catalytic activity of the electrode after water electrolysis and the presence of any electrodeposited material need to be ruled out.

Polyoxometalates (POMs) are a versatile family of inorganic molecular clusters.²² In these complexes, a transition-metal core can be stabilized by discrete metal oxide frameworks, usually tungstate or molybdate in high oxidation state. These inorganic polyanionic ligands are perfectly stable toward oxidative degradation, and their oxo-bridged structure also allows for reversible proton exchange with the solvent, a feature usually combined with the subsequent oxidation steps in the reaction mechanism of WOCs. A tetranuclear ruthenium-based POM was the first purely inorganic species to show WOC activity.^{23,24} Later, it was reported that a single-site ruthenium POM can also catalyze water oxidation.²⁵ In 2010, Hill and co-workers²⁶ reported that $[\text{Co}_4(\text{H}_2\text{O})_2(\text{PW}_9\text{O}_{34})_2]^{10-}$ (Co_4 ; Figure 1)²⁷ is able to catalyze the oxidation of water. This

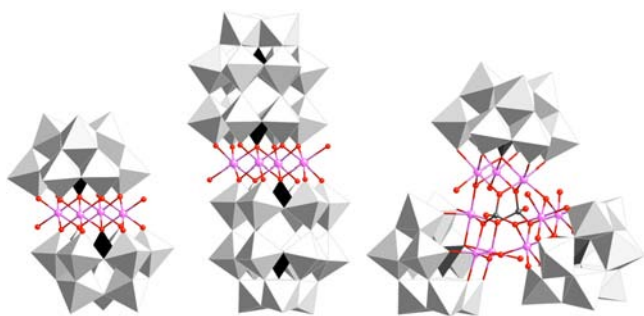


Figure 1. Representation of the molecular structure of the polyanions $[\text{Co}_4(\text{H}_2\text{O})_2(\text{PW}_9\text{O}_{34})_2]^{10-}$ (Co_4 , left), $[\text{Co}_4(\text{H}_2\text{O})_2(\text{P}_2\text{W}_{15}\text{O}_{56})_2]^{10-}$ (Co_4 -Dawson-Wells, center), and $\{\text{Co}_9(\text{H}_2\text{O})_6(\text{OH})_3(\text{HPO}_4)_2(\text{PW}_9\text{O}_{34})_3\}^{16-}$ (Co_9 , right). WO_6 = gray octahedra; PO_4 = black octahedra; Co = pink; P = black; O = red.

WOC represented the first carbon-free homogeneous WOC obtained from abundant metals. It contains a rhomblike tetranuclear cluster of CoO_6 octahedra sharing edges encapsulated by two trivalent Keggin-type $[\text{PW}_9\text{O}_{34}]^{9-}$ units. All bridges between Co atoms are oxo groups, and two terminal water molecules complete the coordination positions.

The activity of Co_4 as a homogeneous WOC has been put into question. It was first reported that it decomposes during electrocatalytic water oxidation to generate a CoO_x film that rapidly becomes the major catalyst.²⁸ More recently, its activity as a catalyst for water chemical oxidation with $[\text{Ru}(\text{bpy})_3]^{3+}$ as the oxidant has also been ruled out.²⁹ Thus, the appearance of cobalt oxide has prevented a precise quantitative characterization of its performance, if any.

Surprisingly, seven other cobalt-containing POMs were tested by Hill's group, but none of them showed any significant activity, although their stability in solution should not differ much from that of Co_4 . Even the Co_4 -Dawson-Wells analogue (Figure 1), with an identical rhomblike tetracobalt active site, was found to be inert. Among all of the POMs tested, the main difference seems to be the pH range in which these polyanions are stable. Co_4 is prepared at the highest pH among them. More recently, another cobalt-containing polymolybdate has been reported as a WOC but with very different structural features.³⁰

We decided to test a cobalt-containing POM with higher nuclearity:³¹ the nonanuclear $\{\text{Co}_9(\text{H}_2\text{O})_6(\text{OH})_3(\text{HPO}_4)_2(\text{PW}_9\text{O}_{34})_3\}^{16-}$ cluster (Co_9 ; Figure 1). This POM is prepared and stable at a higher pH than Co_4 . It forms in a solution of sodium tungstate, sodium phosphate, and cobalt(II) acetate at $\text{pH} > 7$. Its molecular structure³² contains three triads of edge-sharing $\text{Co}^{\text{II}}\text{O}_6$ octahedra supported by three trivalent Keggin-type $[\text{PW}_9\text{O}_{34}]^{9-}$ units. The triads are interconnected through three OH^- and two HPO_4^{2-} bridges. Six of the Co ions complete their coordination sphere with terminal water molecules. The structural differences with Co_4 are (i) a triangle of triangles versus rhombohedral core structure, (ii) the presence of hydroxyl bridges versus only oxo bridges, (iii) available hydrogen phosphate bridges that are not embedded in the POM structure, and (iv) a higher percentage of terminal water molecules. Here, we report the performance of Co_9 as a WOC, carefully avoiding the formation of any other heterogeneous species in turnover conditions.

RESULTS AND DISCUSSION

Characterization of the Electrocatalytic Water Oxidation Activity of Co_9 . We initially carried out bulk water electrolysis experiments under stirring in a two-chamber cell with both chambers connected through a glass frit (Figure S1 in the Supporting Information, SI). As the anode and cathode, we used fluorine-doped tin oxide (FTO) coated glass and platinum mesh electrodes, respectively. Negligible current values were obtained in a $\text{pH} = 7$ sodium phosphate buffer (NaPi , 50 mM) solution with NaNO_3 (1 M) as the electrolyte when an anodic overpotential of ≈ 600 mV was applied (1.41 V vs NHE). With the addition of Co_9 (1 mM) to the anode compartment, the current rapidly increases over 1 order of magnitude, reaching typical values over 3 mA. However, through this process, a brown film slowly deposits on the anode. As oxidation proceeds, the film grows thicker and the current intensity decreases until it reaches a constant value after 1 h. The film was characterized as a cobalt oxide with some phosphate traces, in good agreement with Finke's data.²⁸ We tested the activity of this film with a successive bulk electrolysis using the CoO_x -covered anode in the absence of Co_9 . No significant change in the current is observed (Figure 2), indicating that the deposited cobalt oxide is the main active WOC. The presence of the

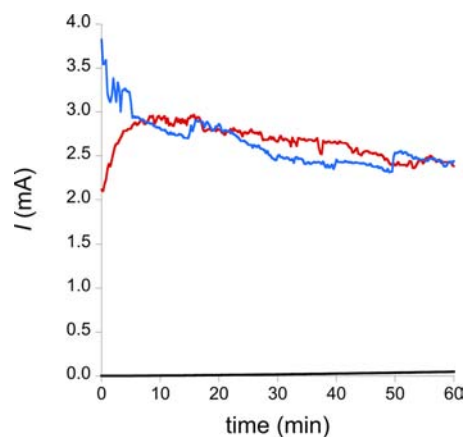
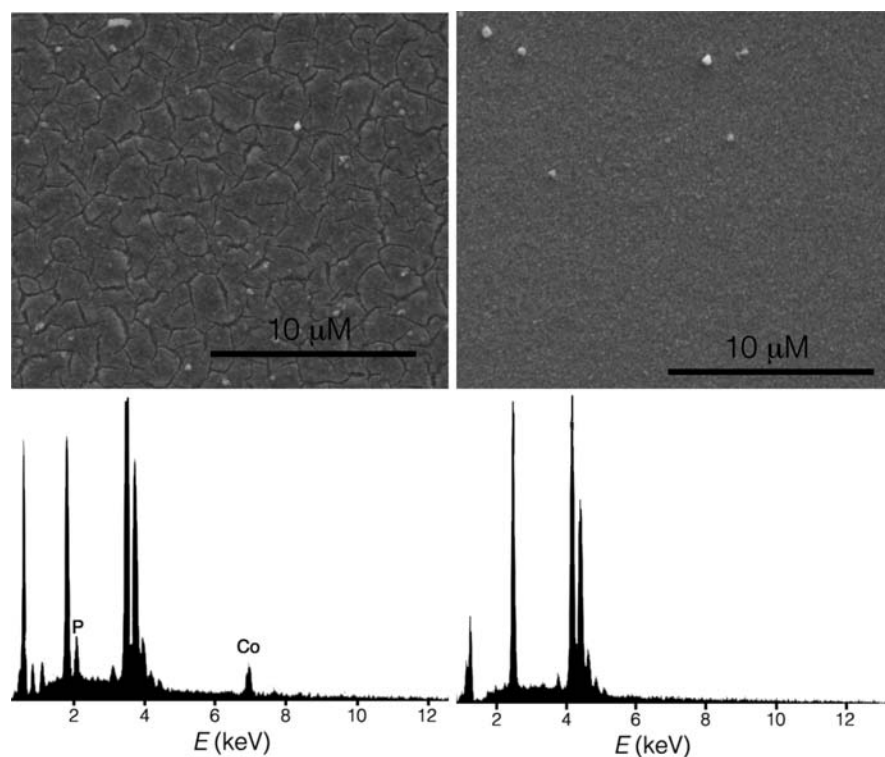


Figure 2. Water electrolysis under an applied voltage of 1.41 V vs NHE in a $\text{pH} = 7$ sodium phosphate buffer (50 mM) water solution with NaNO_3 (1 M) as the electrolyte. Initial blank (black line); 1.0 mM Co_9 (red line); blank after Co_9 -catalyzed electrolysis (blue line).



We determined, with a fluorescence probe, the efficiency for oxygen evolution of this electrocatalytic reaction (Figure S2 in the SI). It is quantitative for the first 15 min, and then it maintains $\approx 90\%$ efficiency for over 1 h. The current not involved in water oxidation probably comes from the expected oxidation of the $[\text{Co}(\text{bpy})_3]^{2+}$ species generated in solution. Indeed, at the end of the catalytic cycle, a fine pink precipitate appeared at the bottom of the reactor. This precipitate was characterized as a $[\text{Co}(\text{bpy})_3]^{3+}$ salt of the Co_9 polyanion. IR spectrometry shows typical spectra of Co_9 , with some additional bands that can be assigned to a tris(bipyridyl)metal complex (Figure S3 in the SI). Metal analysis showed a 1:2 Co/W ratio, consistent with $[\text{Co}^{3+}(\text{bpy})_3]_4\text{A}_4\{\text{Co}_9\}$ stoichiometry, where $\text{A} = \text{Na}^+$ or K^+ (Figure S4 in the SI). This highly insoluble precipitate can also be prepared by the addition of $[\text{Co}(\text{bpy})_3]^{3+}$ to a Co_9 solution.

In cyclic voltammetry measurements, a catalytic water oxidation wave is observed, as expected (Figure S5 in the SI). In the presence of bpy, the current curve deviates from the blank above 1.10 V, as the catalytic water oxidation wave starts. On the contrary, when bpy is not present in solution, the current signal deviates from the blank just above 0.75 V. This voltage is not enough to oxidize water, and this current should be related to the formation of a cobalt oxide film without any water oxidation occurring, as was already stated by Nocera and co-workers.³³ The current increases much faster after 1.10 V, indicating the onset of catalytic water oxidation. The current values are higher than those in the only Co_9 -catalyzed case. These features corroborate again the presence of a cobalt oxide catalyst in this second case and they also completely rule out its participation when a chelating agent is present in solution.

The Tafel plot from steady current density data follows the expected linear trend (Figure 5). For a 1 mM catalyst

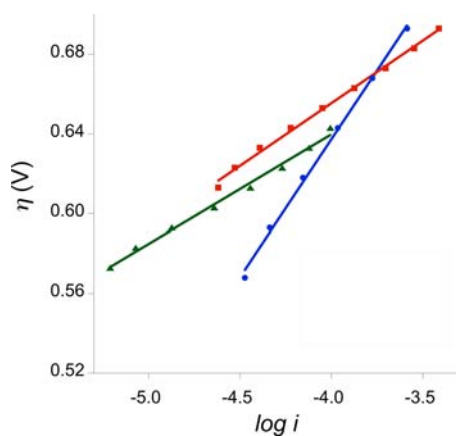


Figure 5. Steady-state Tafel data acquired with FTO anodes in a pH = 7 sodium phosphate buffer (50 mM) water solution with NaNO_3 (1 M) as the electrolyte at different Co_9/bpy concentrations: 1.00/2.80 mM, Tafel slope = $138 \text{ mV decade}^{-1}$ (blue); 0.25/0.68 mM, Tafel slope = $63 \text{ mV decade}^{-1}$ (red); 0.06/0.16 mM, Tafel slope = $55 \text{ mV decade}^{-1}$ (green). Ohmic drop was compensated for using a positive feedback compensation.

concentration, a measurable current density was observed over 1.15 V vs NHE, corresponding to an overpotential $\eta = 353 \text{ mV}$. The calculated Tafel slope is consistently in the $130\text{--}140 \text{ mV decade}^{-1}$ range, measured with different sample batches. This slope implies that the rate-determining step is electrochemical,^{34,35} arising from electron- or mass-transport issues. A

$\eta = 776 \text{ mV}$ would be needed to reach $1 \text{ mA s}^{-1} \text{ cm}^{-2}$. In more dilute conditions, the kinetics of the catalyzed water electrolysis change as the Tafel slope decreases. Below 0.25 mM, the slope is in the $55\text{--}65 \text{ mV decade}^{-1}$ range, consistent with a chemical step becoming the rate-limiting one.^{33,36} Thus, a lower overpotential is needed to reach the same current densities. For example, we found that $\eta = 695 \text{ mV}$ would be needed to reach $1 \text{ mA s}^{-1} \text{ cm}^{-2}$ with a 0.06 mM Co_9 concentration. It needs to be stated that the current densities obtained in these experimental conditions are lower than those observed for cobalt oxides, where an overpotential below 450 mV typically allows one to reach analogous i . It is also worth mentioning that this comparison is not fair to the homogeneous catalyst because the current density is concentration-dependent. Unfortunately, limiting the turnover frequency (TOF) cannot be directly calculated from our electrochemical experiments. Without a noncatalytic redox process, it is difficult to calculate the diffusion layer to determine the number of molecules interacting with the electrode at a given time.^{19,37} Bulk chemical water oxidation is helpful in this regard.

Characterization of the Catalytic Activity of Co_9 with NaClO . When Co_9 is added to a sodium hypochlorite solution with a pH = 8 sodium phosphate buffer [0.9 M], oxygen evolution starts immediately (Figure 6). We confirmed through

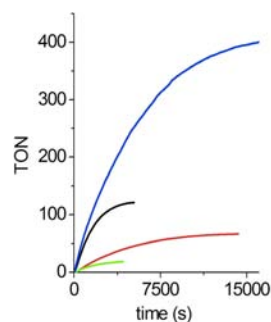


Figure 6. Oxygen evolution profile for a 1.0 mM Co_9 solution after the addition of different equivalents of NaClO as the oxidant (10^2 , green; 10^3 , red; 3.3×10^3 , black; 3.3×10^3 , blue) in a NaPi buffer at pH = 8.0. The reaction was stopped in each case once a constant oxygen partial pressure was reached.

online mass spectrometry (MS) that the gas evolved is exclusively oxygen (Figure S6 in the SI). No traces of any other gas were found. We monitored quantitative oxygen evolution with differential manometry at various oxidant/catalyst ratios. The built-in pressure difference between the blank reaction and after the addition of Co_9 can be converted directly to oxygen equivalents. A maximum turnover number (TON) of 20 is reached for an initial 100:1 oxidant/ Co_9 ratio after 1 h, with an initial TOF over 40 h^{-1} . NaClO is a two-electron oxidant. So, this TON reflects 40% efficiency. This efficiency, far from being quantitative, indicates that there are competing reactions, probably disproportionation of hypochlorite to yield chloride and chlorite (vide infra). The TON and TOF increase dramatically when the oxidant equivalents are increased, whereas the efficiency decreases. For example, a $3.3 \times 10^3:1$ ratio yields a TON of over 400 and an initial TOF of 350 h^{-1} , for a rough efficiency of 2.5%. As expected, higher temperatures improve the dynamics and efficiency of catalysis. The total yield doubles from 15 to $25 \text{ }^\circ\text{C}$, and we found an optimum performance at $35 \text{ }^\circ\text{C}$, with 50% efficiency. Although faster WOCs have been reported, we need to stress that TOF

depends not only on the catalyst but also on the oxidant. Hypochlorite is particularly slow. The fastest WOC for hypochlorite water oxidation showed a much slower TOF of 12 h^{-1} .¹⁸ All of our experiments were repeated at least twice, and the results were confirmed with gas chromatography (GC). The GC and manometry data show excellent agreement. Oxygen evolution data are summarized in Table 1.

Table 1. Manometry Data for Catalytic Oxygen Evolution in a 0.9 M Sodium Phosphate Buffer Solution (pH = 8) with NaClO as the Oxidant, after the Addition of Co_9 at 25°C ^a

$[\text{Co}_9]$ (mM)	oxidant equivalents	$[\text{NaClO}]$ (mM)	reaction time (h)	TON	TOF _i (h^{-1})	TON _{GC}
1	10^2	10^2	1.7	20	42	23
10^{-1}	10^3	10^3	3.5	75	70	72
10^{-1}	3.3×10^3	3.3×10^2	1.4	121	246	
10^{-2}	3.3×10^4	3.3×10^2	5.5	410	351	

^aReaction time refers to the time when oxygen evolution stops; TON = total turnover number at the final reaction time; TOF_i = slope of the oxygen evolution curve at the starting time; TON_{GC} = compared GC data.

When 100:1 catalytic oxidation is performed at pH = 7 or 9, comparable TON numbers are obtained (Figure 7). Some

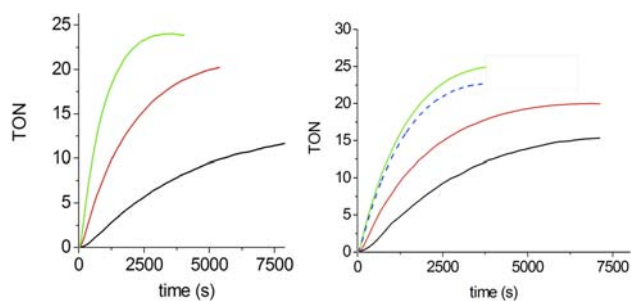


Figure 7. Oxygen evolution profile for a 1.0 mM Co_9 solution after the addition of 100 equivalents of NaClO as the oxidant in a NaPi buffer: (left) as a function of the temperature (15 °C, black; 25 °C, red; 35 °C, green; pH = 8.0); (right) as a function of the pH (7.0, black line; 8.0, red line; 9.0, green line; 9.0 in the presence of a 10-fold excess of bpy, dotted blue line; $T = 25^\circ\text{C}$).

differences are observed for the initial TOFs. The reaction is slower at lower pH, and the catalytic cycle is twice as fast at higher pH. The possible decomposition of Co_9 to yield free Co^{2+} ions into a CoO_x precipitate had to be ruled out. After oxidation, the solutions were studied by UV–vis spectroscopy, where no significant change in the absorbance was detected. Dynamic light scattering (DLS) analysis also ruled out the presence of heterogeneous nanoparticles because identical data were found for the solution before and after oxygen evolution (Figure S7 in the SI). Co_9 can be recovered from solution by recrystallization with additional alkali cations or by slow evaporation of the reaction media. The resulting salt is identical with the starting sample, as was proven by IR spectroscopy and X-ray diffraction (Figures S8 and S9 in the SI). Following our strategy for electrochemical studies, we repeated the experiments, adding a 10-fold excess of bpy per Co atom. The results were consistent. No significant differences in TON or TOF were found in the presence of bpy. Only at pH = 9 was a decrease in these parameters observed. This decrease in activity should be due to decomposition of the POM to a new species

that does not improve the catalytic performance. All of these experimental results confirm that our catalyst is the main active species throughout oxidation. The temperature also has an impact in the catalytic cycle (Figure 7).

We also studied oxygen evolution with ^{18}O -labeled water. When 19.4% H_2^{18}O -labeled water was used as the solvent in the 100:1 reaction, MS analysis of the evolved O_2 showed an accurate agreement with the expected statistical distribution. This suggests that water is the main source for O atoms. However, it has been reported how ClO^- rapidly exchanges the O atom with the solvent and, therefore, this experiment cannot be taken as proof for long reaction times.

Hypochlorite as the Primary Oxidant for WOCs. The water oxidation catalytic activity at neutral pH is an important technological objective. Nevertheless, few homogeneous WOCs work in these conditions. Maybe because of this, most chemical oxidants commonly used for the characterization of new WOCs are only active at very low pH. For example, cerium(IV), a preferred oxidant, precipitates out of solution at $\text{pH} > 3$. We found other typical oxidants such as $[\text{Ru}(\text{bpy})_3]^{3+}$, oxone, and periodate,^{17,38} but no catalytic activity was detected. It has been reported that Co_4 does not react with periodate either, suggesting that it is not a good primary oxidant for POM oxidation catalysts.

We selected sodium hypochlorite as our primary oxidant because it is kinetically inert toward water oxidation, highly soluble, and stable at neutral pH. It was used as a model water oxidant¹⁸ until it was found that ClO^- exchanges the O atom with the solvent, reaching equilibrium at 30 s, for a half-life of about 10 s.¹⁷ This put into question the isotope-labeling experiments required to confirm the source of O atoms. This is a common problem for all oxidants containing oxygen, including the lately accepted periodate that also shows rapid oxo exchange.³⁸ In the case of ClO^- , it has been well established that the main dismutation pathway yields chloride and chlorite, another strong oxidants. The oxygen-evolving pathway is much slower and typically negligible.³⁹



We performed and compared studies of the very initial kinetics of the oxygen-evolving reaction dissolving alternatively the oxidant or catalyst in isotope-labeled water. If water is the main O_2 source, oxygen evolution should be identical in both cases (diffusion control) because the labeled water ratio has the same evolution during oxidation. On the contrary, if ClO^- is the main O_2 source, the initial dynamics should be different (exchange control). For instance, when using 97% ^{18}O -labeled water for preparation of the ClO^- solution, we would have an initial 97% Cl^{18}O^- content. After mixing it with a nonlabeled Co_9 solution, if Cl^{18}O^- is the main O_2 source, we should observe higher $^{34}\text{O}_2$ and $^{36}\text{O}_2$ initial ratios because the Cl^{18}O^- content would actually decrease from its initial maximum value to the 19.4% ^{18}O content at equilibrium, because of exchange with the solvent. When using nonlabeled water for preparation of the ClO^- solution, after mixing it with a 97% ^{18}O -labeled Co_9 solution, we should observe, initially, much slower $^{34}\text{O}_2$ and $^{36}\text{O}_2$ evolution dynamics because the Cl^{18}O^- content would increase up to 19.4% ^{18}O at equilibrium. Although the MS data need a few seconds to become stable, both experiments showed identical $^{32}\text{O}_2$: $^{34}\text{O}_2$: $^{36}\text{O}_2$ dynamic evolution at very short times (<30 s) before equilibrium was reached

(Figure S10 in the SI). According to these results, the most plausible hypothesis is that water is the main O₂ source. Still, as Crabtree concludes, the use of primary oxidants gives solid information on the catalytic water oxidation activity, including rates and stability, even if the real source of oxygen cannot be unambiguously determined.

If water is the main source, the mechanism for oxygen evolution should proceed through a two-step oxidation of the POM by two hypochlorite molecules, probably including proton extraction from the ligated water molecules. The electrons extracted from the Co^{II} centers would generate at least one Co^{IV} center. Also, this would be the active species able to oxidize water. The complex structure of Co₉ precludes a more detailed picture of the mechanism at this time.

Comparison between Co₉ and Co₄ as Chemical Oxidation Catalysts. We carried out the same experiments with Hill's Co₄ catalyst (Table 2). A comparison with our

Table 2. Comparison of Manometry Data for Catalytic Oxygen Evolution in 1 M Sodium Phosphate Buffer Solutions (pH = 8) with NaClO as the Oxidant, after the Addition of Co₉ or Co₄ at 25 °C^a

POM	[Co ₉] (mM)	oxidant equivalents	[NaClO] (mM)	TON	TOF _i (h ⁻¹)
Co ₉	1	10 ²	10 ²	20	42
	10 ⁻¹	10 ³	10 ³	67	70
Co ₄	1	10 ²	10 ²	2	6
	10 ⁻¹	10 ³	10 ³	5	34

^aTON = total turnover number at the final reaction time; TOF_i = slope of the oxygen evolution curve at the starting time.

results puts into perspective the remarkable catalytic performance of Co₉. Co₄ yields only 2 TON (Figure 8) when it is

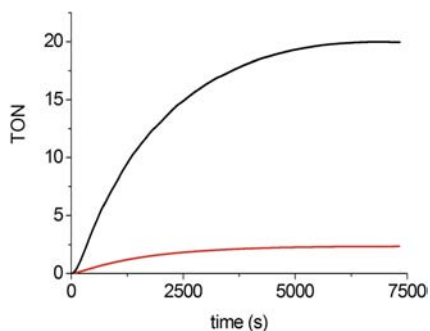


Figure 8. Oxygen evolution profile for 1.0 mM Co₉ (black) and Co₄ (red) solutions, respectively, after the addition of 100 equiv of NaClO as the oxidant in a pH = 8 phosphate buffer solution.

added to a sodium hypochlorite solution in a 100:1 ratio in a NaPi pH = 8 buffer (0.9 M). This corresponds to 4% efficiency. Calculated initial TOF data indicate that Co₉ is at least 8 times faster than Co₄. These differences are maintained for a 1000:1 ratio, giving 75 and 5 TON, respectively, although the initial Co₉ TOF is just twice that of Co₄. Because these experiments were carried out with the same POM concentration, it can be argued that the different cobalt content might account for the observed differences. If we calculate the catalytic activity numbers per Co atom, the superior performance of Co₉ is corroborated, with 2.2 vs 0.5 (7.4 vs 1.3) TON for a 100:1 (1000:1) ratio, although the turns per WOC get closer. From a technological perspective, it is also interesting to compare the

activity per gram of catalyst because not only the Co content is important regarding costs. Taking into account the M_w of the POM salts, we can estimate that 250 and 29 mg of O₂ can be obtained per gram of POM with a 1000:1 oxidant/POM ratio for Co₉ and Co₄, respectively. These data demonstrate that both catalysts show very similar kinetics, with comparable turns per second. On the other hand, the total O₂ yield indicates that Co₉ is much more efficient. This might be related to how robust this POM appears to be in turnover conditions.

Long-Term Stability of Co₉ in Turnover Conditions. In our opinion, Co₉ really surpasses all expectations regarding stability and continuous performance. Once oxygen evolution stops, we added additional equivalents of oxidant or catalyst to determine the limiting reagent. The addition of catalyst did not show any effect. Successive additions of oxidant to the reaction restarted oxygen evolution, maintaining consistent and essentially identical TON and TOF (Table 3). These data

Table 3. Manometry Data for Co₉-Catalyzed Oxygen Evolution in Sodium Phosphate Buffer Solutions (pH = 8) after Successive Additions of NaClO as the Oxidant at 25 °C^a

[Co ₉] (mM)	oxidant equivalents	time of addition (h)	TON	TOF _i (h ⁻¹)	TON _c
10 ⁻¹	10 ³	0	75	70	75
10 ⁻¹	10 ³	2.5	55	69	130
10 ⁻¹	10 ³	5.0	50	67	180
10 ⁻²	3.3 × 10 ⁴	0	148	391	148
10 ⁻²	3.3 × 10 ⁴	1.6	158	379	306
10 ⁻²	3.3 × 10 ⁴	3.0	217	367	523
10 ⁻²	3.3 × 10 ⁴	4.5	200	355	723
10 ⁻²	3.3 × 10 ⁴	6.0	165	343	888
10 ⁻²	3.3 × 10 ⁴	0	255	391	255
8 × 10 ⁻³	3.3 × 10 ⁴	84.0	215	468	470
6 × 10 ⁻³	3.3 × 10 ⁴	108.0	180	586	650
5 × 10 ⁻³	3.3 × 10 ⁴	131.0	173	689	823

^aTON = total turnover number at the next addition or final time; TOF_i = slope of the oxygen evolution curve at the oxidant addition time; TON_c = cumulative TON.

demonstrate that Co₉ remains quantitatively intact in solution once the reaction is complete, as expected. As shown before, the rate and yield of the catalytic oxidation of water with hypochlorite are very sensitive to changes in the oxidant/Co₉ ratio, and a significant decrease in the catalyst concentration would affect the results. Furthermore, decomposition to other species would result in further changes in the catalytic activity, as observed for Co₄.²⁸ The addition of 1000 equiv of oxidant to a Co₉ (0.1 mM) NaPi pH = 8 buffer [0.9 M] solution every 2 h yielded a final cumulative TON of 180 and a constant initial TOF of 69 ± 2 (after three cycles). The addition of 3.3 × 10³ equiv of oxidant every ≈2 h yielded a total cumulative TON > 880 and a constant initial TOF ≈ 370 ± 20 h⁻¹ (after five cycles). The mean TOF over the reaction time holds over 100 h⁻¹.

In order to test the stability limits of Co₉ in solution, we repeated these experiments by adding the additional equivalents of oxidant after longer periods of time (Figure 9) and in the presence of a 10-fold excess of bpy. We found that the Co₉ solution remains completely active for over 1 week, without any sign of fatigue or decomposition. To the best of our knowledge, no other reported WOC can remain active for such a long time

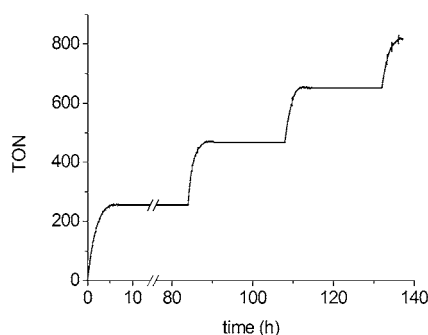


Figure 9. Oxygen evolution profile in 1 M sodium phosphate buffer solutions (pH = 8) after successive additions of NaClO as the oxidant at 25 °C.

either under chemical, electrochemical, or photoinduced water oxidation conditions. Oxygen evolution data for all of these stability tests are shown in Table 3.

CONCLUSIONS

We have discovered the catalytic activity of a novel cobalt-containing POM, the $\{\text{Co}_9(\text{H}_2\text{O})_6(\text{OH})_3(\text{HPO}_4)_2(\text{PW}_9\text{O}_{34})_3\}^{16-}$ polyanion (Co_9). We have demonstrated that this nonanuclear cobalt cluster stabilized by a polyoxophosphotungstate moiety is a true homogeneous WOC at neutral pH. As an electrocatalyst, its decomposition to yield a thin cobalt oxide film on the anode can be easily avoided by the addition of chelating agents. Our experimental data confirm that catalytic water oxidation occurs in the absence of any heterogeneous species generated in situ, and Co_9 can be recovered from solution after the catalytic cycles. In diluted conditions, it shows kinetic features similar to those of cobalt oxides at reasonable overpotentials. Furthermore, Co_9 is amazingly stable and robust in chemical water oxidation experiments. It is able to catalyze oxygen evolution from a sodium hypochlorite solution in the $7 < \text{pH} < 9$ range for days, without any sign of fatigue or decomposition. We have shown how weeks old Co_9 solutions present activity identical with that of freshly prepared ones, even after multiple cycles of catalytic oxidation. All our data corroborate that Co_9 is a viable candidate to be incorporated into an artificial photosynthesis device.

EXPERIMENTAL SECTION

All reagents were purchased from Sigma-Aldrich (>99% purity) and used without further purification. A sodium hypochlorite solution was bought from Sigma-Aldrich (16% free chlorine). The metal content in POM catalysts was analyzed with a JEOL-JMS6400 environmental scanning electron microscope equipped with an Oxford Instruments X-ray elemental analyzer. Thermogravimetric analysis (TGA) was performed with power samples using a TGA/SDTA851 Mettler Toledo with a MT1 microbalance. UV–vis spectroscopy was performed on a Cary 50 (Varian) spectrophotometer in standard 1 cm quartz cuvettes. Single-crystal X-ray diffraction was performed with a Bruker-Nonius diffractometer equipped with an APEX2 4K CCD area detector, a FR591 rotating anode with Mo $K\alpha$ radiation, Montel mirrors as the monochromator, and a Kryoflex low-temperature device. Powder X-ray diffraction data were collected with a Bruker D8 Advance Series equipped with a VA NTEC-1 PSD detector.

Synthesis and Characterization. The Co_4 and Co_9 POMs were prepared from optimized literature methods.^{27,31} The recrystallized solids were collected by filtration and dried in vacuum. The counteranions and solvent content were determined by energy-dispersive analysis of X-rays (EDAX) microanalysis and TGA,

respectively. The molecular formulas are $\text{Na}_5\text{K}_5[\text{Co}_4(\text{H}_2\text{O})_2(\text{PW}_9\text{O}_{34})_2]\cdot 31\text{H}_2\text{O}$ ($M_w = 5599.7$) and $\text{Na}_8\text{K}_8[\text{Co}_9(\text{OH})_3(\text{H}_2\text{O})_6(\text{HPO}_4)_2(\text{PW}_9\text{O}_{34})_3]\cdot 43\text{H}_2\text{O}$ ($M_w = 8842.6$). The compounds were also characterized by spectroscopy and powder X-ray diffraction. Identical spectroscopic and structural data were found for Co_9 samples recovered after water oxidation. Single-crystal X-ray diffraction (Bruker-Nonius diffractometer FR591 with an APEX2 4K CCD detector) confirmed consistent unit cells: $P6_3/m$, $a = 20.243(3)$ Å, $c = 20.343(4)$ Å, and $V = 7220$ Å³ (before) and $P6_3/m$, $a = 20.701(6)$ Å, $c = 20.399(5)$ Å, and $V = 7571$ Å³ (recrystallized after oxidation catalysis), both isostructural and in agreement with the reported data.³² The small unit cell differences found are due to different water and alkali cation contents.

Physical Methods. UV–vis spectroscopy was performed on a Cary 50 (Varian) UV–vis spectrophotometer in standard 1 cm quartz cuvettes. TGA measurements were performed with a MT1-type TGA/SDTA851 Mettler Toledo microbalance. Microanalysis was performed with a JEOL-JSM6400 scanning electron microscope equipped with an Oxford EDAX analyzer (Oxford Instruments). DLS data were obtained with a Malvern nanoZS analyzer.

Electrochemistry. Bulk water electrolysis was carried out with stirring in a two-chamber cell, with a porous frit connecting both chambers. In one chamber, we placed a platinum mesh counter electrode, and in the other chamber, we placed a FTO-coated glass working electrode and a Ag/AgCl (3 M NaCl) reference electrode. Data were collected with a Biologic SP-150 potentiostat. Typical electrolysis experiments were carried out in a NaPi buffer pH = 7 solution with NaNO_3 (1 M) as the electrolyte. Tafel data were gathered in the same experimental conditions, taking as stable current data after 10 min of electrolysis. The ohmic drop was compensated for using the positive feedback compensation implemented in the instrument. Oxygen evolution was determined with an Ocean Optics NeoFOX oxygen-sensing system equipped with a FOXY probe inserted into the anodic compartment.

Manometric Measurements. A gas evolution profile of catalytic experiments was monitored by a Testo 521 manometer, with an internal differential pressure sensor from 0 to 100 hPa and accuracy within 0.2% of the measurement. One manometer port was connected to a thermostatted vessel for the online monitoring of the headspace pressure above the catalysis reaction. The other manometer port was connected to a thermostatted vessel containing the same solvent and headspace volume as the sample vial. In a typical catalyzed reaction, 2 mmol of catalyst dissolved in 1.8 mL of a 1 M phosphate buffer solution at pH = 8.0 was introduced in a vessel, and the pressure was stabilized. Then, a solution of 200 mmol of NaClO (100 equiv) in 0.2 mL of a phosphate buffer was added to the initial solution. The entire system was thermostatted at the desired temperature between 15 and 35 °C.

GC Measurements. The oxygen content was determined by using an Agilent 6890N gas chromatograph with a thermal conductivity detector. In a typical experiment, the desired amount of catalyst was introduced in a 10 mL round-bottomed flask, and it was extensively degassed under cycles of vacuum and nitrogen for 30 min. Then, the catalyst was dissolved in 9 mL of a degassed phosphate buffer solution at pH = 8.0. After this, 1 mL of a degassed 1 M NaClO solution was added in order to start catalysis. Samples of 200 μL from the generated gas phase in the reaction flask headspace were taken with a 250 μL Hamilton gastight syringe and immediately injected into the instrument for analysis. Calibration of the method was carried out by employing the previous procedure, using water instead of the reaction mixture. A calibration slope was obtained by the addition of different quantities of oxygen (0, 5, 10, 20, and 30 μmol of O_2) in the headspace of the reaction flask. After each addition, gas and aqueous phases were stirred until equilibrium was achieved. The integrated data peaks were correlated with the amount of oxygen added. The slope from the integrated data points was employed for quantification of oxygen in the catalysis experiments carried out.

¹⁸O Labeling. All solutions were degassed prior to use. In a typical procedure, 2 mmol of the complex was dissolved in 1.4 mL of a phosphate buffer solution at pH = 8.0 and introduced into a flask.

Then water oxidation catalysis was performed by adding 100 equiv of NaClO in a mixture of 0.2 mL of phosphate buffer and 0.4 mL of H₂¹⁸O (water ¹⁸O, 97%, Cambridge Isotope Laboratories, Inc.). The final ratio of solvent labeled was 19.4% in this case. The same experiment was also performed by dissolving the catalyst in H₂¹⁸O and the oxidant in water and at different H₂¹⁸O/H₂¹⁶O ratios. The composition of the gas phase (¹⁶O₂, *m/z* 32; ¹⁶O¹⁸O, *m/z* 34; ¹⁸O₂, *m/z* 36) was monitored online by an Omnistar GSD 301 C (Pfeiffer) quadrupole mass spectrometer apparatus. All solutions were prepared in such a way that they contained a final 0.9 M phosphate buffer solution at pH = 8.0.

■ ASSOCIATED CONTENT

Supporting Information

Additional experimental data including MS, spectroscopy, labeling experiments, and X-ray diffraction. This material is available free of charge via the Internet at <http://pubs.acs.org>.

■ AUTHOR INFORMATION

Corresponding Author

*E-mail: jrgalan@iciq.es.

Notes

The authors declare the following competing financial interest(s): Authors in this manuscript are co-inventors of a patent application (EP11382322) on the use of the Co₉ catalyst and related POMs for water oxidation.

■ ACKNOWLEDGMENTS

We are thankful for financial support of the EU (ERC Stg Grant CHEMCOMP), the Spanish Ministerio de Ciencia e Innovación (Grant CTQ2008-03197), and the ICIQ Foundation. We thank Prof. Jean-Michel Savéant and Prof. Antoni Llobet for helpful discussion. We also thank Dr. J. Benet, Dr. E. C. Escudero, Dr. M. Martínez, and Dr. E. Martin from the X-ray Diffraction Unit at ICIQ for their help in the X-ray diffraction experiments and Dr. M. González-Hevia from the Heterogeneous Catalysis Unit at ICIQ for his help in the MS and DLS experiments.

■ REFERENCES

- (1) (a) Lewis, N. S.; Nocera, D. G. *Proc. Natl. Acad. Sci. U.S.A.* **2006**, *103*, 15729–15735. (b) Balzani, V.; Credi, A.; Venturi, M. *ChemSusChem* **2008**, *1*, 26–58.
- (2) Mirzakułova, E.; Khatmullin, R.; Walpita, J.; Corrigan, T.; Vargas-Barbosa, N. M.; Vyas, S.; Oottikkal, S.; Manzer, S. F.; Hadad, C. M.; Glusac, K. D. *Nat. Chem.* **2012**.
- (3) (a) Kern, J.; et al. *Proc. Natl. Acad. Sci. U.S.A.* **2012**, *109*, 9721–9726. (b) Mukherjee, S.; Stull, J. A.; Yano, J.; Stamatatos, T. C.; Pringouri, K.; Stich, T. A.; Abboud, K. A.; Britt, R. D.; Yachandra, V. K.; Christou, G. *Proc. Natl. Acad. Sci. U.S.A.* **2012**, *109*, 2257–2262. (c) Umena, Y.; Kawakami, K.; Shen, J.-R.; Kamiya, N. *Nature* **2011**, *473*, 55–60. (d) Ferreira, K. N.; Iverson, T. M.; Maghlaoui, K.; Barber, J.; Iwata, S. *Science* **2004**, *303*, 1831–1838.
- (4) Mills, A. *Chem. Soc. Rev.* **1989**, *18*, 285–316.
- (5) (a) Kanan, M. W.; Nocera, D. G. *Science* **2008**, *321*, 1072–1075. (b) Hocking, R. K.; Brimblecombe, R.; Chang, L.-Y.; Singh, A.; Cheah, M. H.; Glover, C.; Casey, W. H.; Spiccia, L. *Nat. Chem.* **2011**, *461*–466. (c) Maeda, K.; Ohno, T.; Domen, K. *Chem. Sci.* **2011**, *2*, 1362–1368. (d) Jiao, F.; Frei, H. *Angew. Chem., Int. Ed.* **2009**, *48*, 1841–1844. (e) Yagi, M.; Tomita, E.; Sakita, S.; Kuwabara, T.; Nagai, K. *J. Phys. Chem. B* **2005**, *109*, 21489–21491.
- (6) (a) Cowan, A. J.; Barnett, C. J.; Pendlebury, S. R.; Barroso, M.; Sivula, K.; Grätzel, M.; Durrant, J. R.; Klug, D. R. *J. Am. Chem. Soc.* **2011**, *133*, 10134–10140. (b) Sivula, K.; Le Formal, F.; Grätzel, M. *ChemSusChem* **2011**, *4*, 432–449. (c) Alexander, B. D.; Kulesza, P. J.; Rutkowska, I.; Solarska, R.; Augustynski, J. *J. Mater. Chem. Soc.* **2008**,

18, 2298–2303. (d) Mohapatra, S. K.; John, S. E.; Banerjee, S.; Misra, M. *Chem. Mater.* **2009**, *21*, 3048–3055.

- (7) Pijpers, J. J. H.; Winkler, M. T.; Surendranath, Y.; Buonassisi, T.; Nocera, D. G. *Proc. Natl. Acad. Sci. U.S.A.* **2011**, *108*, 10056–10061.
- (8) Nocera, D. G. *Acc. Chem. Res.* **2012**, *45*, 767–776.
- (9) (a) Van Noorden, R. *Nat. News* **2012**, DOI: 10.1038/nature.2012.10703. (b) Minguzzi, A.; Fan, F.-R. F.; Vertova, A.; Rondinini, S.; Bard, A. J. *Chem. Sci.* **2012**, *3*, 217–229.
- (10) Liu, X.; Wang, F. Y. *Coord. Chem. Rev.* **2012**, *1115*–1136.
- (11) Concepcion, J. J.; Jurss, J. W.; Brennaman, M. K.; Hoertz, P. G.; Patrocinio, A. O. T.; Murakami Iha, N. Y.; Templeton, J. L.; Meyer, T. J. *Acc. Chem. Res.* **2009**, *42*, 1954–1965.
- (12) Gersten, S. W.; Samuels, G. J.; Meyer, T. J. *J. Am. Chem. Soc.* **1982**, *104*, 4029–4030.
- (13) (a) Sens, C.; Romero, I.; Rodriguez, M.; Llobet, A.; Parella, T.; Benet-Buchholz, J. *J. Am. Chem. Soc.* **2004**, *126*, 7798–7799. (b) Bozoglian, F.; Romain, S.; Ertem, M. Z.; Todorova, T. K.; Sens, C.; Mola, J.; Rodriguez, M.; Romero, I.; Benet-Buchholz, J.; Fontrodona, X.; Cramer, C. J.; Gagliardi, L.; Llobet, A. *J. Am. Chem. Soc.* **2009**, *131*, 15176–15187. (c) Romain, S.; Bozoglian, F.; Sala, X.; Llobet, A. *J. Am. Chem. Soc.* **2009**, *131*, 2768–2769. (d) Concepcion, J. J.; Jurss, J. W.; Templeton, J. L.; Meyer, T. J. *J. Am. Chem. Soc.* **2008**, *130*, 16462–16463. (e) Xu, Y.; Fischer, A.; Duan, L.; Tong, L.; Gabrielson, E.; Akermark, B.; Sun, L. *Angew. Chem., Int. Ed.* **2010**, *49*, 8934–8937.
- (14) (a) Blakemore, J. D.; Schley, N. D.; Balcells, D.; Hull, J. F.; Olack, G. W.; Incarvito, C. D.; Eisenstein, O.; Brudvig, G. W.; Crabtree, R. H. *J. Am. Chem. Soc.* **2010**, *132*, 16017–16029. (b) Lairempuia, R.; McDaniel, N. D.; Muller-Bunz, H.; Bernhard, S.; Albrecht, M. *Angew. Chem., Int. Ed.* **2010**, *49*, 9765–9768.
- (15) (a) McCool, N. S.; Robinson, D. M.; Sheats, J. E.; Dismukes, G. C. *J. Am. Chem. Soc.* **2011**, *133*, 11446–11449. (b) Wasylenko, D. J.; Ganesamoorthy, C.; Borau-Garcia, J.; Berlinguette, C. P. *Chem. Commun.* **2011**, *47*, 4249–4251.
- (16) (a) Lloret-Fillol, J.; Codolé, Z.; García-Bosch, I.; Gómez, L.; Pla, J. J.; Costas, M. *Nat. Chem.* **2011**, *3*, 807–813. (b) Ellis, W. C.; McDaniel, N. D.; Bernhard, S.; Collins, T. J. *J. Am. Chem. Soc.* **2010**, *132*, 10993–10991.
- (17) Limburg, J.; Vrettos, J. S.; Chen, H. Y.; de Paula, J.; Crabtree, G. W.; Brudvig, R. H. *J. Am. Chem. Soc.* **2001**, *123*, 423–430.
- (18) Limburg, J.; Vrettos, J.; Liable-Sands, L.; Rheingold, A.; Crabtree, R.; Brudvig, G. *Science* **1999**, *283*, 1524–1527.
- (19) Barnett, S. M.; Goldberg, K. L.; Mayer, J. M. *Nat. Chem.* **2012**, *4*, 498–502.
- (20) (a) Hintermair, U.; Hashmi, S. M.; Elimelech, M.; Crabtree, R. H. *J. Am. Chem. Soc.* **2012**, *134*, 9785–9795. (b) Hong, D.; Murakami, M.; Yamada, Y.; Fukuzumi, S. *Energy Environ. Sci.* **2012**, *5*, 5708–5716. (c) Hong, D.; Jung, J.; Park, J.; Yamada, Y.; Suenobu, T.; Lee, Y.-M.; Nam, W.; Fukuzumi, S. *Energy Environ. Sci.* **2012**, *5*, 7606–7616.
- (21) Schley, N. D.; Blakemore, J. D.; Subbairam, N. K.; Incarvito, C. D.; D'Souza, F.; Crabtree, R. H.; Brudvig, G. W. *J. Am. Chem. Soc.* **2011**, *133*, 10473–10481.
- (22) (a) Long, D. L.; Burkholder, E.; Cronin, L. *Chem. Soc. Rev.* **2007**, *36*, 105–121. (b) Hill, C. L. *J. Mol. Catal. A: Chem.* **2007**, *262*, 2–6. (c) Kortz, U.; Mueller, A.; van Slageren, J.; Schnack, J.; Dalal, N. S.; Dressel, M. *Coord. Chem. Rev.* **2009**, *253*, 2315–2327.
- (23) (a) Sartorel, A.; Carraro, M.; Scorrano, G.; De Zorzi, R.; Geremia, S.; McDaniel, N. D.; Bernhard, S. e.; Bonchio, M. *J. Am. Chem. Soc.* **2008**, *130*, 5006–5007. (b) Sartorel, A.; Miro, P.; Salvadori, E.; Romain, S.; Carraro, M.; Scorrano, G.; Di Valentin, M.; Llobet, A.; Bo, C.; Bonchio, M. *J. Am. Chem. Soc.* **2009**, *131*, 16051–16052.
- (24) (a) Geletii, Y. V.; Botar, B.; Koegerler, P.; Hillesheim, D. A.; Musaev, D. G.; Hill, C. L. *Angew. Chem., Int. Ed.* **2008**, *47*, 3896–3899. (b) Besson, C.; Huang, Z.; Geletii, Y. V.; Lense, S.; Hardcastle, K. I.; Musaev, D. G.; Lian, T.; Proust, A.; Hill, C. L. *Chem. Commun.* **2010**, *46*, 2784–2786. (c) Toma, F. M.; et al. *Nat. Chem.* **2010**, *2*, 826–831.
- (25) Murakami, M.; Hong, D.; Suenobu, T.; Yamaguchi, S.; Ogura, T.; Fukuzumi, S. *J. Am. Chem. Soc.* **2011**, *133*, 11605–11613.

- (26) Yin, Q.; Tan, J. M.; Besson, C.; Geletii, Y. V.; Musaev, D. G.; Kuznetsov, A. E.; Luo, Z.; Hardcastle, K. L.; Hill, C. L. *Science* **2010**, *328*, 342–345.
- (27) Weakley, T. J. R.; Evans, H. T.; Showell, J. S.; Tourne, G. F.; Tourne, C. M. *J. Chem. Soc., Chem. Commun.* **1973**, 139–140.
- (28) Stracke, J. J.; Finke, R. G. *J. Am. Chem. Soc.* **2011**, *133*, 14872–14875.
- (29) Natali, M.; Berardi, S.; Sartorel, A.; Bonchio, M.; Campagna, S.; Scandola, F. *Chem. Commun.* **2012**, *48*, 8808–8810.
- (30) Tanaka, S.; Annaka, M.; Sakai, K. *Chem. Commun.* **2012**, *48*, 1653–1655.
- (31) Galán-Mascarós, J. R.; Gómez-García, C. J.; Borrás, J. J.; Coronado, E. *Adv. Mater.* **1994**, *6*, 221–223.
- (32) Weakley, T. J. R. *J. Chem. Soc., Chem. Commun.* **1984**, 1406–1407.
- (33) Surendranath, Y.; Kanan, M. W.; Nocera, D. G. *J. Am. Chem. Soc.* **2010**, *132*, 16501–16509.
- (34) Gerken, J. B.; McAlpin, J. G.; Chen, J. Y. C.; Rigsby, M. L.; Casey, W. H.; Britt, R. D.; Stahl, S. S. *J. Am. Chem. Soc.* **2012**, *133*, 14431–14442.
- (35) Dau, H.; Limberg, C.; Reier, T.; Risch, M.; Roggan, S.; Strasser, P. *ChemCatChem* **2010**, *2*, 724–761.
- (36) Pijpers, J. J. H.; Winkler, M. T.; Surendranath, Y.; Buonassisi, T.; Nocera, D. G. *Proc. Natl. Acad. Sci. U.S.A.* **2011**, *108*, 10056–10061.
- (37) Costentin, C.; Drouet, S.; Robert, M.; Savéant, J.-M. *J. Am. Chem. Soc.* **2012**, *134*, 11235–11242.
- (38) Parent, A. R.; Brewster, T. P.; DeWolf, W.; Crabtree, G. W.; Brudvig, R. H. *Inorg. Chem.* **2012**, *51*, 6147–6152.
- (39) (a) Lister, M. W. *Can. J. Chem.* **1956**, *34*, 479–488. (b) Lister, M. W.; Petterson, R. C. *Can. J. Chem.* **1962**, *40*, 729–733. (c) Adam, L. C.; Gordon, G. *Inorg. Chem.* **1999**, *38*, 1299–1304.